Energy & Buildings 279 (2023) 112680

Contents lists available at ScienceDirect

Energy & Buildings

journal homepage: www.elsevier.com/locate/enb

Experimental study of PCM-enhanced building envelope towards energy-saving and decarbonisation in a severe hot climate

Qudama Al-Yasiri [a,b,c,*], Márta Szabó [b]

[a] Doctoral School of Mechanical Engineering, Hungarian University of Agriculture and Life Sciences, Szent István Campus, Páter K. u. 1, Gödöllő H-2100, Hungary
[b] Department of Building Engineering and Energetics, Institute of Technology, Hungarian University of Agriculture and Life Sciences, Szent István Campus, Páter K. u. 1, Gödöllő H-2100, Hungary
[c] Department of Mechanical Engineering, Faculty of Engineering, University of Misan, Al Amarah City, Maysan Province 62001, Iraq

ARTICLE INFO

Article history:
Received 28 September 2022
Revised 15 November 2022
Accepted 17 November 2022
Available online 21 November 2022

Keywords:
PCM-integrated buildings
Indoor temperature reduction
Heat gain reduction
CO_2 emission saving
Building energy-saving

ABSTRACT

Phase change materials (PCMs)-enhanced building envelope has received much attention in recent years as an effective solution to enhance building thermal performance. Nevertheless, minimal experimental studies considering PCM influential aspects in full envelope arrangement are found in the literature against many numerical studies. This paper aims to quantify the indoor temperature improvement and energy-saving when PCM is passively-incorporated into a building envelope under non-ventilated conditions. The average indoor temperature reduction (AITR), thermal load levelling reduction (TLLR), average heat gain reduction (AHGR) and associated CO_2 emissions saving (CO_2 ES) and energy cost saving (ECS) are presented and discussed for two test rooms, with/without PCM, constructed and examined in extremely hot summer days. The outcomes exhibited PCM effectiveness to stabilise the indoor temperature, showing an AITR of 2 °C during the day and a maximum TLLR of 8.71 %. Besides, AHGR by up to 56 W, CO_2 ES by 1.35 kg/day and ECS of 80.64 Iraqi dinar (IQD)/day are attained. The study concluded that the PCM is more effective in the roof than walls, and the PCM amount should vary in walls considering their orientation and peak outdoor conditions.

1. Introduction

The building sector is the most alarming energy consumer worldwide due to population growth, rapid urbanisation and high thermal comfort standards of occupants in modern society [1]. The International Energy Agency (IEA) stated that buildings are the major global energy consumer, wherein the building envelope was responsible for 36 % of final energy consumption and 39 % of carbon dioxide (CO_2) emissions in 2018 [2]. Therefore, different techniques should be practically-applied to improve the building envelope performance towards better energy-saving and decarbonisation in the built environment, especially in poor-acting buildings in hot locations [3].

Incorporating phase change materials (PCMs) with building elements is among the fast-growing technologies nowadays, thanks to their high potential for thermal energy storage and flexible use to amend building energy-saving and thermal comfort [4]. PCMs can effectively work as a dynamic heat barrier in hot-location buildings by preventing unwanted heat during the daytime and releasing it at night. Likewise, they can act as a heat source in cold-location buildings by storing diurnal heat and using it to support heating demand.

Literature studies have verified different applications of PCMs in building elements, including walls [5], floors [6], windows [7], roofs [8], cladding [9] and plastering [10]. In this regard, Kishore et al. [11] investigated different PCM types using a dynamic wall system under various locations numerically. The main outcomes indicated that PCM-integrated walls could reduce heat gain by 15 %–72 % annually, influenced by the building location. Qu et al. [12] performed a numerical study to show the energy-saving and thermal comfort of buildings under the Chinese climate by considering four factors, namely the PCM type, the PCM layout, the PCM layer thickness and the envelope type. Results revealed that the factors influenced the building performance according to the following descending order: type of envelope > PCM layout > PCM type > PCM thickness. Among investigated PCMs, BioPCM^{TM}23 was optimal at 7 cm thickness on the inside of walls and roof, showing energy-saving by 4.8 % – 34.8 %. The PCM melting temperature (Tm), PCM layer position and quantity are the most influential factors of PCM integration. In this regard, Tunçbilek et al. [13]

* Corresponding author.
E-mail addresses: qudamaalyasiri@uomisan.edu.iq, qudamaalyasiri@uomisan.edu.iq (Q. Al-Yasiri), Szabo.marta@uni-mate.hu (M. Szabó).

https://doi.org/10.1016/j.enbuild.2022.112680
0378-7788/

Nomenclature

AIT	Average indoor temperature [°C]
AITR	Average indoor temperature reduction [%]
AHGR	Average heat gain reduction [W]
CO_2	Carbon dioxide
CO_2 ES	CO_2 emission saving [kg/m^3.day]
ECS	Electricity cost saving [IQD/m^3.day]
HG	Heat gain [W]
IEA	International Energy Agency
IQD	Iraqi dinar
PCM	Phase change material
TLL	Thermal load levelling
TLLR	Thermal load levelling reduction [%]
Tm	Melting temperature [°C]

Symbols

A	Area [m^2]
h	Convective-radiative heat transfer coefficient for the interior element surface and interior room temperature [W/m^2.K]
$HG_{PCM\ element}$	Heat gain of the PCM element [W]
$HG_{Ref\ element}$	Heat gain of the reference element [W]
$T_{i,PCM\ room,av}$	Average indoor air temperature of the PCM room [°C]
$T_{i,Ref\ room,av}$	Average indoor air temperature of the reference room [°C]
$T_{i,Ref\ room,max}$	Maximum indoor air temperature of the reference room [°C]
$T_{i,Ref\ room,min}$	Minimum indoor air temperature of the reference room [°C]
$T_{i,PCM\ room,max}$	Maximum indoor air temperature of the PCM room [°C]
$T_{i,PCM\ room,min}$	Minimum indoor air temperature of the PCM room [°C]
τ	Time [min]

studied an office building wall performance when integrated with PCMs in Turkey based on various PCM transition temperatures, different layer positions and thicknesses. To this aim, they studied eleven PCMs of various Tm ranging from 20 °C to 30 °C and PCM layer thickness (5 to 30 mm) with different PCM layer positions varied from the outdoor to the indoor. Numerical results exhibited the best thermal performance of the PCM of 25 °C Tm irrespective of the PCM layer thickness. Besides, in the best case, the PCM at 23 mm showed the best performance when placed near the indoor environment and can save 12.8 % more energy than the reference case, the wall without PCM. Hamidi et al. [14] explored the benefits of incorporating PCMs into hollow brick walls in eight Mediterranean regions for cooling demand reduction. Several PCMs of Tm varied between 22 °C and 32 °C were considered for three building types: single-family, collective housing and hotel housing, by applying an apparent heat capacity numerical model via COMSOL Multiphysics software. They found that the climate has the most significant influence on the PCM effectiveness, and up to 56 % energy saving could be reached with a PCM of 26 °C Tm in the North-East Mediterranean cities regardless of the building type. Rathore and Shukla [15] experimentally quantified the peak temperature reduction, temperature time lag and electricity saving when integrating PCM with the building envelope (namely roofs and walls) under Indian conditions. The results indicated peak temperature reduction by 40.67 %-59.79 %, time lag extension by 60–120 min and electrical energy saving by ∼0.40 US $/day. Al-Rashed et al. [16] numerically studied the heat gain obtained from incorporating a 20 mm PCM layer in building envelope (roof and walls) considering three different PCMs (RT-31, RT-35 and RT-42) under Kuwait climate conditions. The study found that the higher the PCM Tm, the better the thermal performance of the building envelope. Therefore, incorporating RT-42 has reduced the heat gain of the roof by 15.37 % and that of walls by 13.78 %, respectively, compared with the reference case. Moreover, the findings showed that RT-31 could minimise CO_2 emissions by 98.65–481 kWh/m^2. year in worst cases. Li and Shi [17] studied the energy-saving of mortar-based composite paraffin/expanded vermiculite-diatomite for wall application. The results showed temperature reduction and energy-saving of wall-based composite PCM by respectively 2.68 °C and 17.03 % compared with the pristine mortar. Saxena et al. [18] conducted experimental work under Delhi (India) climate conditions to investigate the PCM thermal performance when incorporated into bricks by single and dual capsules. The results indicated a temperature reduction of 4 °C and 9.5 °C with single and dual PCM capsules, along with a heat transfer reduction of 40 %-60 % across bricks during peak hours. Ye et al. [19] numerically researched the potential of passive PCMs to enhance the thermal performance of prefabricated temporary houses, considering the thermal comfort hours and energy-saving annually. They also evaluated the influence of PCM thickness, PCM Tm, building orientation, ventilation effect, and climatic region. The numerical findings revealed that the PCM thickness affected the house performance in various regions. Furthermore, the thermal comfort period was increased from 803 h to 1511 h when the wall composition changed from 100 mm insulation board to 90 mm insulation boards plus 10 mm PCM thickness panels. The building orientation had no influence on the optimal PCM type whereas the optimal PCM was different with/without air-conditioning. Besides, the ventilation remarkably enhanced the thermal comfort and abridged the energy consumption in most regions.

Al-Absi et al. [20] experimentally investigated the thermal performance of microencapsulated PCM (Tm = 35 °C) coupled cement render and foamed concrete for exterior wall finishing. The experiment was conducted for test cells with 300 cm^3 size under controlled indoor conditions to study the effectiveness of PCM in reducing indoor and surface temperatures. The results indicated that the peak internal surface temperature was minimised by up to 3.95 °C and heat flux reduced by 26 W/m^2. Therefore, the indoor temperature of the tested cell was reduced by 3.05 °C compared with a reference cell. Ben Zaid et al. [21] tested a composite PCM (40 % polyethylene and 60 % paraffin) panel integrated into a clay-straw wall (80 % clay and 20 % straw) under Moroccan climate conditions. The authors investigated the wall's inner surface temperature and heat flux reduction considering PCM repositioning within the wall. Findings showed that the inner surface temperature could be reduced by 3 °C along with peak heat flux reduction by 31.95 % compared to the pristine clay-straw wall without PCM. The study further revealed that the PCM panel position could lower the inside surface temperature of a wall by 1 °C when placed next to the heat source compared with the outer wall position.

Zhu et al. [22] evaluated the temperature reduction of experimental rooms, one of them coupled shape-stabilised PCM on the south wall under Wuhan city summer conditions in China. Results showed that the PCM wall inside surface temperature was reduced by a maximum of 2.4 °C (0.5 °C on average) for the experimental period from 10th July to 3rd September. Besides, the indoor tem-

perature of the PCM room was reduced by a maximum of 1.9 °C (0.6 °C on average) compared with the other reference room. Berardi and Soudian [23] experimentally compared the thermal performance of a PCM room provided with hybrid PCM (two PCMs of Tm = 21.7 °C and 25 °C) into the roof and walls with another baseline room under Canadian weather conditions. Study findings revealed that the indoor temperature in the PCM was stabilised, even during extreme conditions with a high-temperature variation. In this regard, the indoor and inside surface temperatures were lowered by up to 6 °C at peak time, representing a remarkable thermal performance of hybrid PCM.

The above literature analysis indicates that most PCM-enhanced building studies were verified numerically considering the impact of PCM Tm, influential position and best thickness (quantity) on the building performance. In contrast, limited studies that consider full-scale experimental rooms can be found since most of them focused on PCM-integrated walls only due to the difficulty of experimental set-up considering all influential factors mentioned above. Besides, experimental studies mostly adopted ready-manufactured PCM products (macroencapsulated panels or costly-fabricated microencapsulation PCMs), with the least investigated locally available materials for PCM macroencapsulation. In addition, literature studies were often conducted under moderate weather conditions in contradiction of no highlights of high Tm PCM thermal performance in severe hot climates, leaving an incomplete vision of PCM effectiveness in such locations. Therefore, the current study attempts to experimentally evaluate the performance of a PCM-enhanced full building envelope (roof and walls) as a passive strategy toward energy-saving and decarbonisation in a severe hot climate. In the PCM room, the best incorporation factors, based on follow-up experimental studies, were considered, such as the optimal PCM thickness [24] and position [25] within the roof and the best PCM brick arrangement for walls [26]. The study delivered several aspects to quantify the indoor temperature enhancement and energy-saving, giving a broad vision of the PCM application compared with another reference room.

2. Test rooms and measurements

2.1. Test rooms

Two cubical rooms of 1 m^3 were constructed and tested under hot climate conditions in Al Amarah city (Latitude: 31.84° and Longitude: 47.14°), Iraq, for three consecutive days from 12 to 14.09.2021. One of these rooms incorporated PCM into the roof and walls (called PCM room), whereas the other room was left without PCM for control (referred to as Ref. room). Roofs and walls were constructed from popularly-available construction materials with thicknesses presented in Table 1. Rooms were built on a building's rooftop with an east-south orientation in an open environment and placed on a woody foundation to ensure no exchange of heat between the indoor environment and the rooftop. Besides, a wooden-framed single-glazed window with 250 × 350 mm size was positioned on the east wall of each room. The experimentation was performed under non-ventilated conditions by keeping the windows closed during the whole period. Therefore, the ambient temperature is the only factor controlling heat exchange between indoor and outdoor environments. The final test rooms are shown in Fig. 1.

Although these materials are available at low prices and have good mechanical properties for long-lifetime constructions, they suffer from poor thermal performance in summer due to their high thermal conductivity, resulting in high heat gain [27].

Table 1
Construction materials of experimental rooms.

Construction material	Thickness (mm)
Roof (from outside to inside)	
Isogam (roofing layer)	4
Concrete (main layer)	50
gypsum mortar (cladding layer)	2
Walls (from outside to inside)	
Cement mortar	20
Concrete bricks	230 × 120 × 70
Floor	
Plywood sheet	50

2.2. PCM preparation

Petroleum-based paraffin wax was employed as a PCM in this study. This type of paraffin is a waste product produced in Iraqi refineries during de-waxing. It was selected as a PCM in the study due to its availability in huge quantities in Iraq, which could be employed for sustainable development technologies. The PCM has several desired properties that allow it to be used as a thermal energy storage medium, including its high thermal energy storage capacity, sharp melting and solidification temperatures, safe use and economic concerns. Besides, the Tm range of this paraffin lies within the daily temperature range of the location under study, which guarantees full PCM melting/solidification thermal cycles. It is worth revealing that this PCM type was investigated by local researchers in different applications, including solar heating [28], solar photovoltaics [29], solar desalination [30], and electrical transformers [31], showing interesting advantages. The main thermo-physical characteristics of used paraffin wax are shown in Table 2.

The PCM was macroencapsulated using metal containers and incorporated into the roof and walls of the PCM room. In this regard, a galvanised steel panel was used for macroencapsulation in the roof with 15 mm thickness and 1000 × 1000 mm dimensions. In contrast, aluminium capsules were used for PCM macroencapsulation for walls with 4 × 4 × 2 cm dimensions for each capsule (5 PCM capsules/brick). The PCM panel was incorporated as a separate layer in the roof between the Isogam and concrete layer [25], while the PCM capsules were dipped within the concrete bricks of the PCM room's walls. The PCM quantity/thickness inside the panel and capsules was determined previously considering a series of preliminary experiments. For instance, the PCM panel with 15 mm thickness resulted in the best thermal behaviour

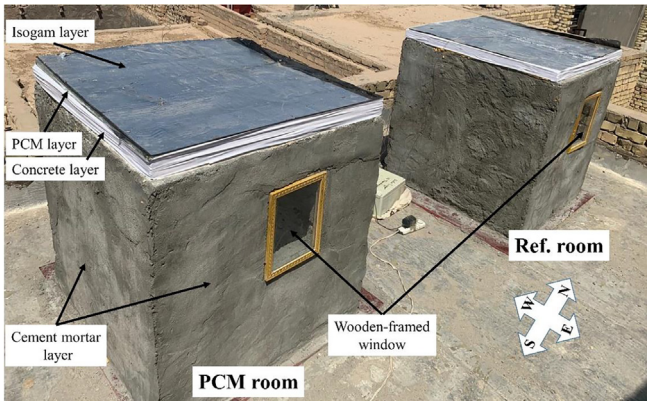

Fig. 1. Test rooms.

Table 2
Thermal and physical properties of used paraffin wax [32,33].

Appearance	Melting temperature (°C)	Thermal conductivity (W/m.K)	Latent heat of fusion (kJ/kg)	Density (kg/m^3)	Specific heat (kJ/kg.K)	Enthalpy (kJ/kg)
Whitish	40–44	0.21	190	930 (solid) 830 (liquid)	2.1	232

compared with 10 and 20 mm considering several energy indicators [24]. Besides, the PCM quantity integrated into each PCM brick was about 45 g and was determined concerning the brick size and capsule number, considering the brick's mechanical strength [26,34]. Some photos of the PCM panel and capsules fabrication are shown in Fig. 2.

2.3. The instrumentation for measurement

The temperature variation was monitored using *T*-type thermocouples connected to a controlled multi-channel Arduino (type Mega 2560), shown in Fig. 3-a. The thermocouples (TEMPSENS brand) have 0.2 mm bare head (non-insulated) of temperature range from −270 °C to 370 °C and a resolution of ± 0.5 °C. This thermocouple type is sensitive to temperature variation with minimal error due to its direct contact with the measured surface. One thermocouple was fixed at the interior centre surface of roofs and walls (Fig. 3-b) using rubber epoxy glue to ensure precise surface temperature measurement with minimal influence on indoor temperature. Besides, one thermocouple was placed at the centre space of each experimental room to measure the indoor temperature variation during cycles. Moreover, two thermocouples were placed outside the rooms at a suitable level to measure the outdoor ambient temperature variation throughout the experimental days. The Arduino was set with 30 min time step, providing data twice per hour. Collected temperatures were stored instantly into detachable flash memory built-up with the Arduino. The solar radiation during day hours was measured every 30 min using a mobile solar power meter (type SM206) with 0.1 W/m^2 resolution, ±10 W/m^2 accuracy and 0.1 ∼ 399.9 W/m^2 measurement range.

3. Results and discussion

The experimental study persisted for three consecutive days, starting from 6:00 on 12.09.2021 till 6:00 on 15.09.2021, under severe hot summer climate conditions in Al Amarah city, southern Iraq. This city has a subtropical desert climate according to the Köppen-Geiger classification. The weather in this city is harsh during the summer season and characterised by high ambient temperatures during the day and night, exceeding the mark of 48 °C and 30 °C, respectively (Fig. 4-a), requiring high-performance air-conditioning systems all day long. Besides, summer days are usually sunny (more than 29 days/month) with a clear sky and high solar radiation (Fig. 4-b). The latest reports stated that Al Amarah city had the hottest climate in Iraq during the summer of 2021 and amongst the highest recorded high ambient temperatures in the Middle East [24].

3.1. Analysis of temperature variation

Figs. 5–10 illustrate the variation of the interior surface temperature of roofs and walls, in addition to the indoor temperature, of the PCM room against those of the reference room, ambient temperature and solar radiation.

In general, the temperature trend was the same every day except for some differences in the temperature values, influenced by varying solar radiation and ambient temperature each day. This trend indicates a positive PCM incorporation impact into the PCM elements since the melting and solidification phases were verified. In other words, the PCM was solidified in the PCM elements by the end of every cycle to be ready for a new cycle the following day. The maximum ambient temperature was recorded at midday in

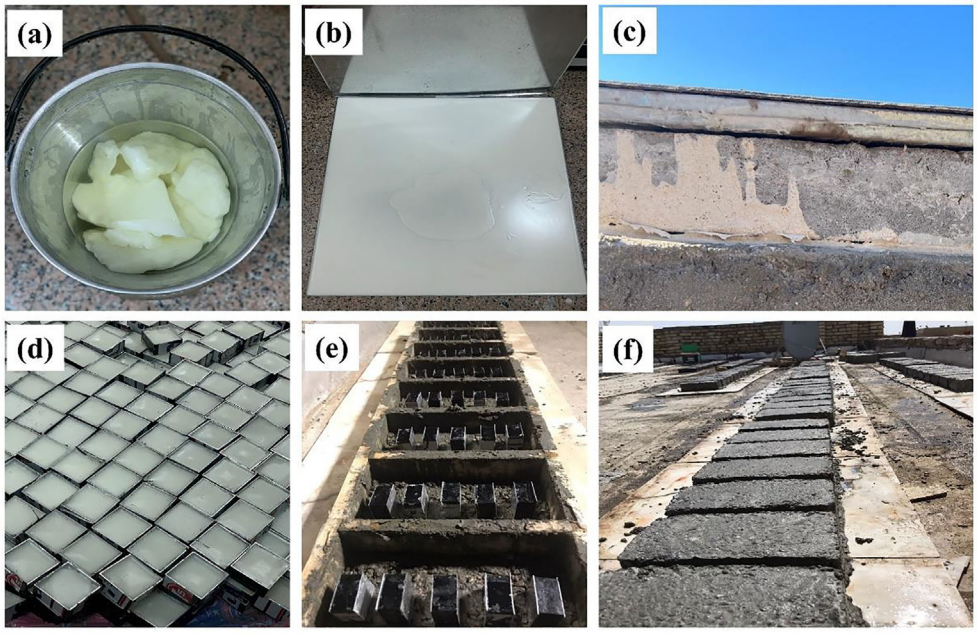

Fig. 2. Site photos of (a) melting paraffin wax (PCM), (b) PCM panel, (c) PCM panel incorporated in the roof, (d) PCM capsules (before capping), (e) PCM capsules inside bricks (during preparation), (f) PCM concrete bricks (wet).

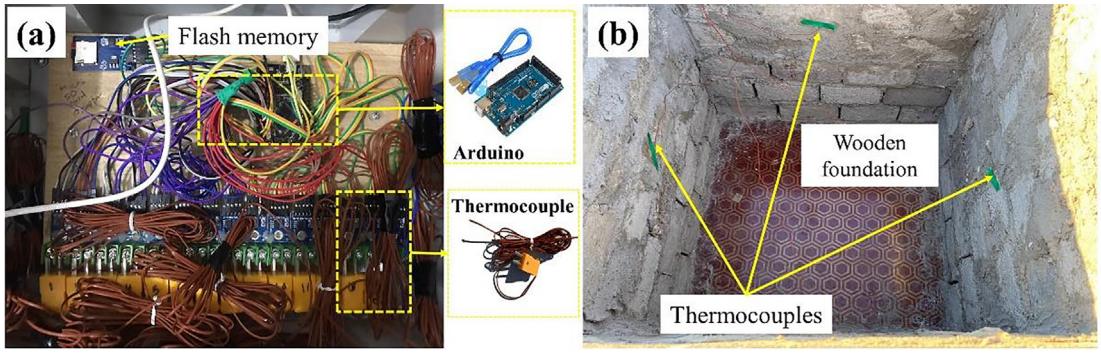

Fig. 3. (a) Data logger, (b) position of thermocouples on inside walls.

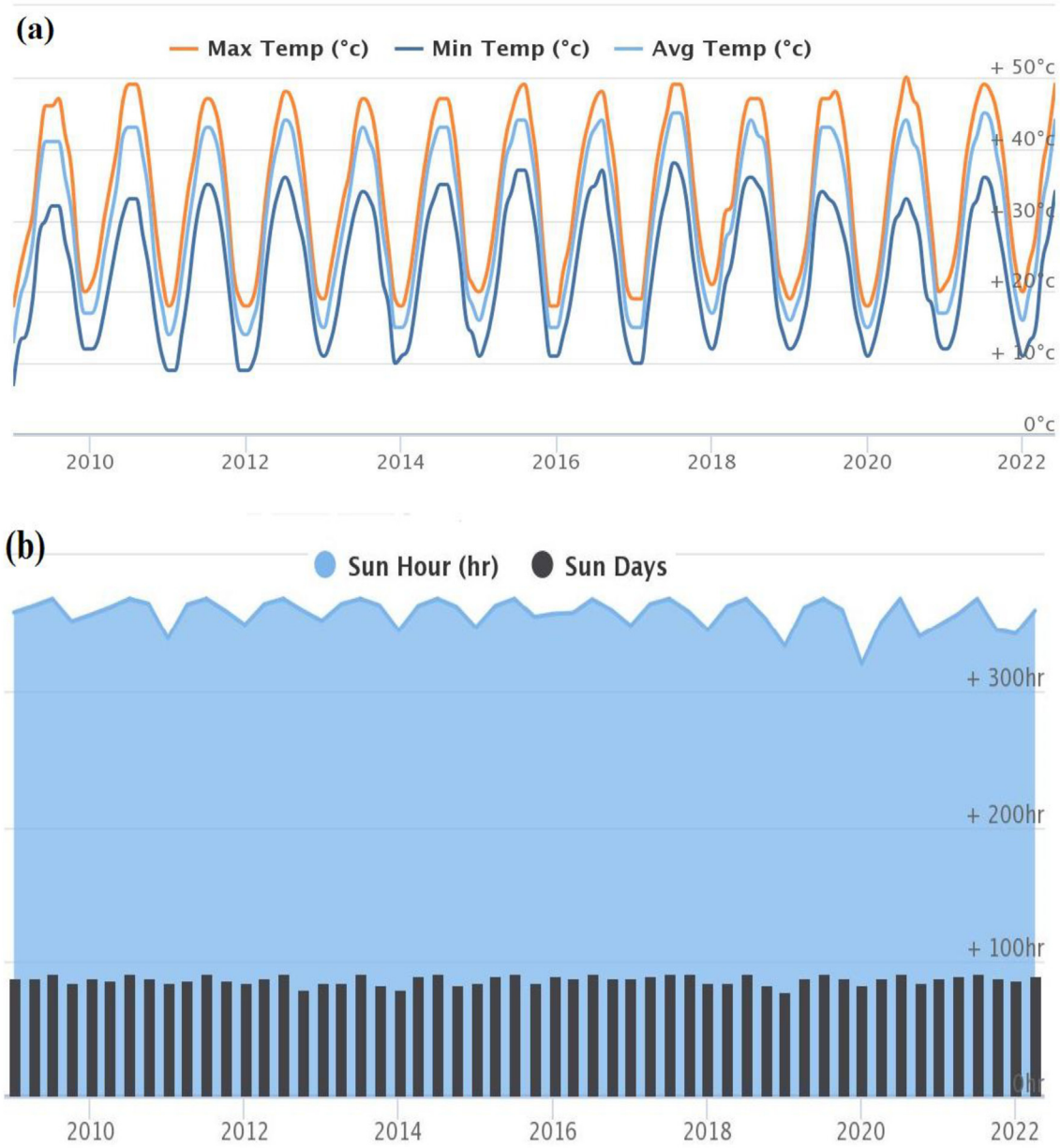

Fig. 4. Historical weather data of Al Amarah city, Iraq from 2009 to 2022 (a) maximum, minimum and average ambient temperature, (b) sun hours and days [35].

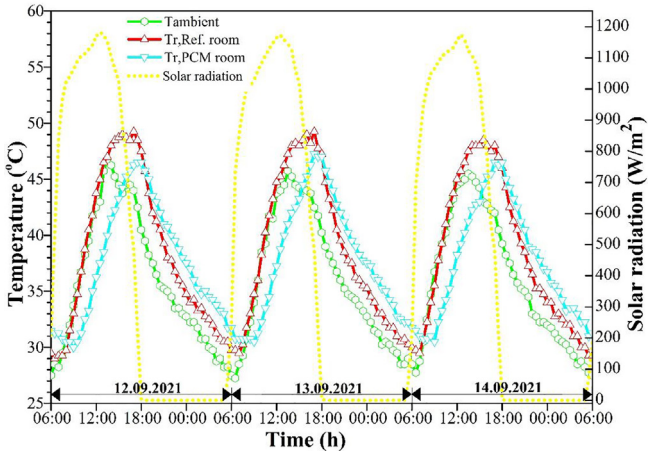

Fig. 5. Surface temperature of roofs against ambient temperature and solar radiation.

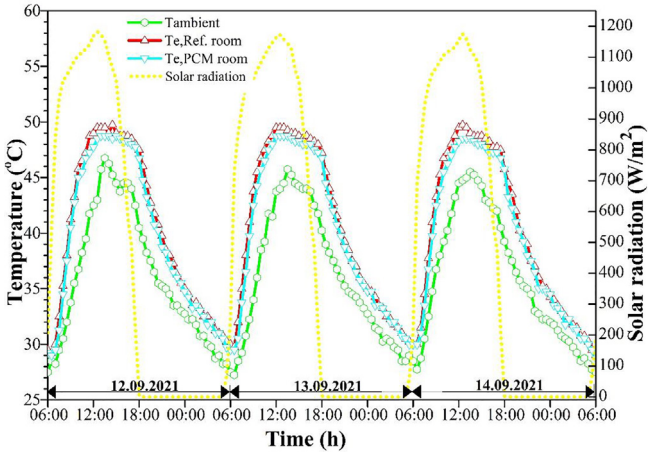

Fig. 6. Surface temperature of east walls against ambient temperature and solar radiation.

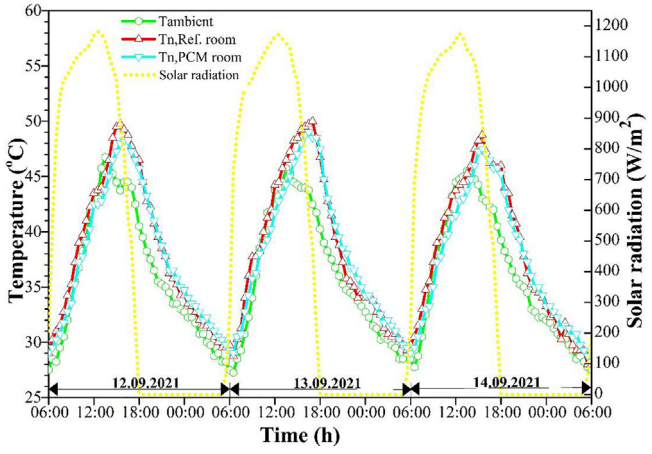

Fig. 7. Surface temperature of north walls against ambient temperature and solar radiation.

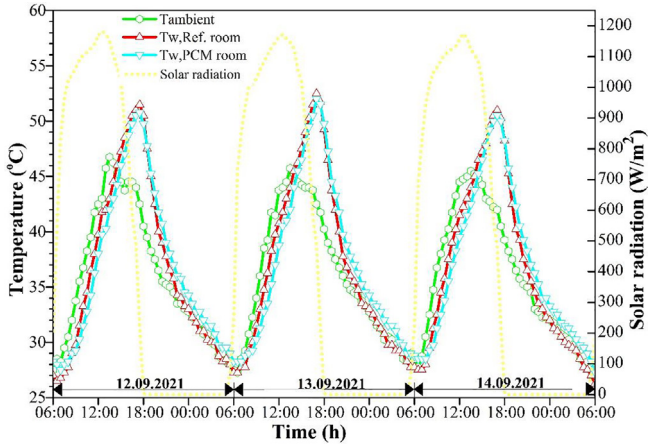

Fig. 8. Surface temperature of west walls against ambient temperature and solar radiation.

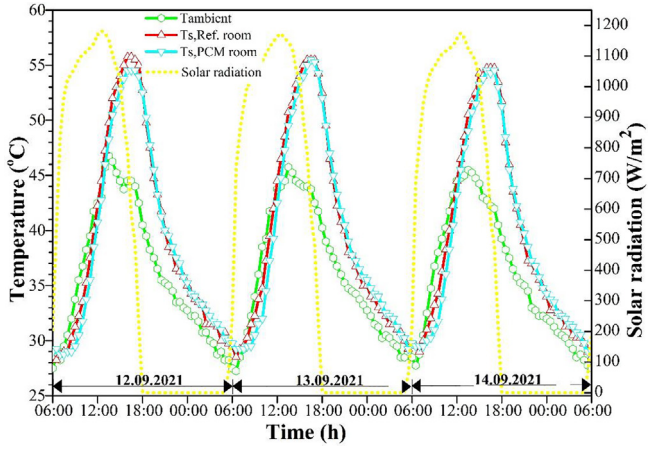

Fig. 9. Surface temperature of south walls against ambient temperature and solar radiation.

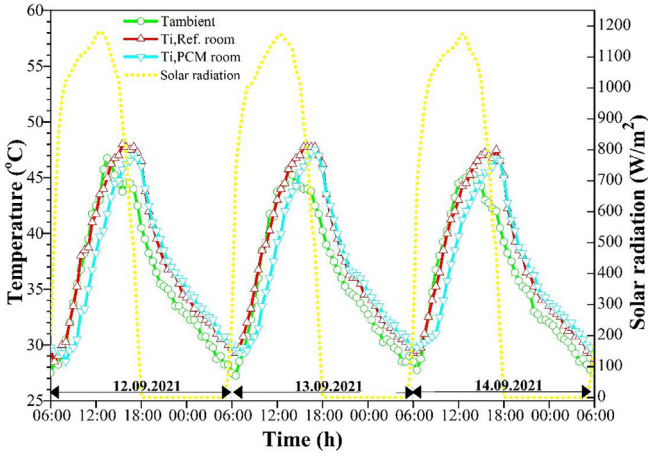

Fig. 10. Indoor temperature against ambient temperature and solar radiation.

conjunction with the highest solar radiation each day. Besides, the maximum surface temperature of PCM and reference elements were recorded with a time lag due to the thermal resistance of element layers, especially in the roof case. The PCM elements showed longer temperature time lag thanks to the incorporated PCM of low-thermal conductivity, which delimited heat flow compared with the reference room. However, the PCM elements showed a negative temperature trend during nighttime compared with the reference elements due to the solidification phase, which began

in the late afternoon, increasing the surface temperature of PCM elements. This may evidence the necessity of incorporating PCM far from the indoor environment in passive building applications under hot locations [36].

It can be seen from the figures that the roofs showed better thermal performance than walls, where the inside surface temperature was noticeably low. The maximum surface temperature of the reference roof was 49.25 °C, 49 °C and 48.5 °C in the first, second and third cycle, respectively, in contradiction to 46.5 °C, 47.25 °C and 46.5 °C for the PCM roof. This temperature difference is mainly attributed to the thick PCM layer in the roof and encapsulation method compared with the walls, not to mention the thermal resistance of roof layers. Furthermore, it is known that the PCM is more beneficial and activates at high temperatures, which is the case of the roof since it is exposed to high-rate solar radiation for a longer time than walls.

East walls (Fig. 6) showed good temperature variation for the inside surface temperature during midday when the solar radiation reached its maximum values after 11:00. The maximum measured inside surface temperature reached the mark of 48.75 °C in the PCM east wall against 49.75 °C in the reference wall. This temperature trend was similar to the south walls (Fig. 9), except that the south walls were exposed to high solar radiation for a longer time, increasing the surface temperature considerably. In this regard, the south walls (Fig. 9) showed high inside surface temperature compared with other walls exceeding the mark of 55 °C since they received high beam solar radiation during the peak period in midday. However, the temperature difference between the PCM and reference walls was relatively good during the whole day hours, showing good thermal performance of the PCM even at high temperatures.

North walls (Fig. 7) showed limited temperature behaviour in the PCM room compared with the reference one since the solar radiation was low in the early morning hours in each cycle. Later on, the north walls were only influenced by the ambient air increased temperature. The highest inside surface temperature recorded in the reference north wall reached 49.5 °C, 49.75 °C and 48.75 °C against 48.75 °C, 49 °C and 47.5 °C recorded in the PCM wall during the thermal cycles. From the other side, the west walls (Fig. 8) showed modest temperature improvement during day hours, with a temperature difference varying between 0.25 °C and 0.75 °C for the PCM west wall compared with the reference wall. These walls are exposed to solar radiation all late afternoon when the PCM capsules have already reached their Tm due to hot air temperature during the day.

The indoor temperature behaviour (Fig. 10) showed the effect of the combined inside surface temperature of all elements, which was more remarkable in the PCM room than in the reference room. For instance, the highest indoor temperature of the reference room in the first thermal cycle was 48 °C at 15:30 compared with 45.75 °C in the PCM room, resulting in a temperature difference of about 2.25 °C. However, the temperature behaviour was adverse in the night hours due to the influence solidification phase of the PCM in a non-ventilated space, as highlighted previously.

In general, it can be stated that the temperature behaviour of PCM walls was time-dependent concerning the sun position and solar radiation rate fall on the wall. Accordingly, the east PCM wall was best in the first half of the day, the south PCM wall was active at noon, while the west PCM wall performed better in the afternoon. Therefore, the PCM wall is more effective as long as it is exposed to high solar radiation. The PCM wall can benefit from PCM potential during phase transition, during which the corresponding reference wall experience worse thermal behaviour. Accordingly, the east PCM wall showed the best temperature behaviour at midday compared with other walls, whereas the west wall activated better in the late afternoon. On the other hand, the PCM was not as efficient in the north PCM wall as in other walls due to low incident solar radiation in the early hours of the day.

3.2. Enhancement of indoor temperature

The enhancement of the indoor environment is a superior aim of incorporating PCM into building elements since it influences occupants' thermal comfort. The indoor temperature improvement in this work was evaluated by considering the indoor temperature for the PCM and reference rooms in terms of the average indoor temperature reduction and thermal load levelling.

3.2.1. Average indoor temperature reduction

The average indoor temperature reduction (AITR) of the PCM room in comparison with the Ref room was presented considering the average indoor air temperature throughout the day hours only (i.e., from 06:00 to 18:00 of each day), according to Eq. (1), as follows:

$$AITR = \sum_{\tau=18:00}^{\tau=06:00} \frac{T_{i,Refroom,av} - T_{i,PCMroom,av}}{T_{i,Refroom,av}} \times 100\% \quad (1)$$

where $T_{i,Ref\ room,av}$ and $T_{i,PCM\ room,av}$ are the average indoor air temperature of the reference and PCM rooms (in °C), respectively, from 06:00 to 18:00. The AITR and average indoor temperature (AIT) of both rooms over thermal cycles is shown in Fig. 11.

The figure indicated lower AIT in the PCM room than in the reference room in all thermal cycles. The AIT of the reference room was 40.13 °C, 40.71 °C and 40.65 °C on the first, second and third day against 37.82 °C, 38.41 °C and 38.56 °C in the PCM room, respectively. The temperature difference between the two rooms was 2.31 °C in the first cycle, 2.3 °C in the second and 2.09° C in the third cycle. Therefore, the AITR varied between 5.14 % and 5.81 % during the experiment period. This improvement represents a remarkable benefit from the thermal comfort perspective since it reduces the power required for air-conditioning systems.

3.2.2. Thermal load levelling

The thermal load levelling (TLL) index indicates how the indoor environment's temperature fluctuates during the day, considering the maximum and minimum indoor temperatures. Therefore, the lower TLL indicates better building envelope thermal performance to stabilise the indoor temperature. The TLL for reference and PCM rooms was calculated according to Eq. (2) and (3) [37], as follows:

$$TLL_{Refroom} = \frac{T_{i,Refroom,max} - T_{i,Refroom,min}}{T_{i,Refroom,max} + T_{i,Refroom,min}} \quad (2)$$

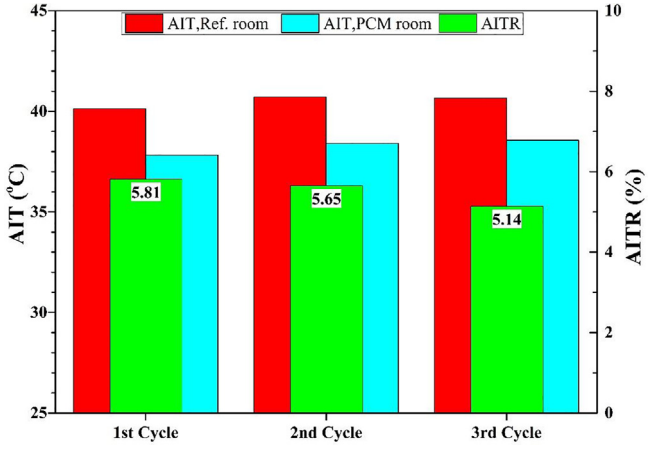

Fig. 11. AIT and AITR in reference and PCM rooms.

$$TLL_{RCMroom} = \frac{T_{i,PCMroom,max} - T_{i,PCMroom,min}}{T_{i,PCMroom,max} + T_{i,PCMroom,min}} \quad (3)$$

The calculation results of TLL and TLL reduction (TLLR) are shown in Fig. 12.

The calculation results of TLL designated that the PCM room has better performance in which the TLL was always lower than the reference room. The TLL in the reference room was 0.23, 0.24 and 0.25 against 0.21, 0.22 and 0.23 in the PCM room during the three thermal cycles. This indicates that the indoor temperature inside the PCM room was more stable than in the reference room throughout the experimental days. The TLL was stable between the two rooms with an index of 0.02 difference. The TLLR was 8.71 %, 8.11 % and 7.28 %, respectively, in the thermal cycles. It is worth mentioning that the TLL difference between the experimental rooms initially resulted from the temperature time lag of the building envelope elements. In other words, the elements of the PCM room had a longer time lag than those of the reference room (evident in Figs. 5–9), thanks to the incorporated PCM, which resulted in a longer time lag in the indoor temperature as well as lower temperature levels (Fig. 10).

3.3. Energy, CO_2 emissions and electricity cost saving

The benefits owing of incorporating PCM into building elements can be evaluated in different concepts. In this work, energy-saving in terms of heat gain reduction, CO_2 emission and electricity cost saving were discussed for this purpose.

3.3.1. Heat gain reduction

The heat gain (HG) is a significant indicator of a building's thermal resistance against the heat flow from the outdoor towards the indoor environment. It has a predominant role in quantifying the cooling energy requirements in the air-conditioning design calculations and system sizing. The HG for every element of the reference and PCM rooms was calculated using Eq. (4) as follows:

$$HG = h_i A \Delta T \quad (4)$$

where h_i is the overall convective/radiative heat transfer coefficient for inside elements and indoor air temperatures. This value was taken as 8.29 W/m^2.°C for walls and 6.13 W/m^2.°C for roofs, bearing in mind the emissivity of 0.9 for concrete structures according to ASHRAE [38]. A is the element area (1 m^2). ΔT is the difference between the inside surface average temperature of a specific element and indoor air temperature (in °C).

The average heat gain reduction (AHGR) was calculated (in W) to compare the HG of elements in the PCM and reference rooms according to Eq. (5), as follows:

$$AHGR = HG_{Ref\ \ element} - HG_{PCM\ \ element} \quad (5)$$

Fig. 13 shows the AHGR results of PCM room elements compared with those of the reference room.

Fig. 13 indicated a similar trend of HG over the three thermal cycles and resulted in near total AHGR by about 54, 56 and 54.7 W in the first, second and third thermal cycles, respectively. The HG of elements corresponding to their temperature behaviour (described in 3.1) regarding time dependence. In other words, the maximum HG of each wall was associated with the time the solar radiation hit that wall. For instance, the maximum AHGR was 14.5 W at 9:00 for the north wall, 12.4 W at 11:30 for the east wall, 14.5 W at 12:30 for the south wall, 14.5 W at 14:00 for the west wall and 45.9 W at 12:30 for the roof. However, the AHGR of each element showed different results since the average value of element HG for the day hours from 6:00 to 18:00 was considered.

As shown in Fig. 13, the roof showed high AHGR compared with the walls, sharing about 22.3 W, 22.1 W and 21.9 W in the first, second and third cycles, respectively. This high AHGR attributes to the high PCM amount integrated into the PCM roof, which stored more heat than the walls. Besides, the roof was exposed to high solar radiation for a long time (compared with walls), making the reference roof thermally poor compared with the PCM roof. This is obvious in Fig. 5, where the PCM required a long solidification period to be ready for the following thermal cycle.

For the case of walls, the east wall exhibited AHGR of 5.6, 6.8 and 6.5 W during the thermal cycles, which is poor compared with the AHGR of other walls. In contrast, the south wall resulted in AHGR by 8.5, 9 and 8.5 W during the experimental days, indicating better thermal performance than the east walls, although the inside surface temperature of the south walls was too high (Fig. 9). This temperature behaviour is affected by sun location, amount of solar radiation during the day and its influence on the room elements. During peak hours of the day, the higher direct solar radiation hits the eastern walls. This activates the PCM inside the PCM wall more quickly, resulting in better temperature reduction at midday than in the reference wall. It is worth highlighting that the windows fixed on the east wall of the experimental rooms had a certain contribution to the overall HG in each room since the single glass pane has a low thermal resistance value and high solar heat gain coefficient [27]. However, the HG of the window is expected to be slight compared to opaque elements (walls and

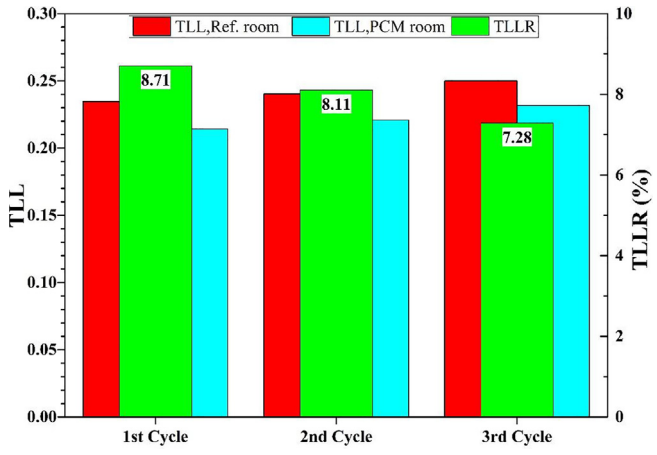

Fig. 12. TLL and TLLR in reference and PCM rooms.

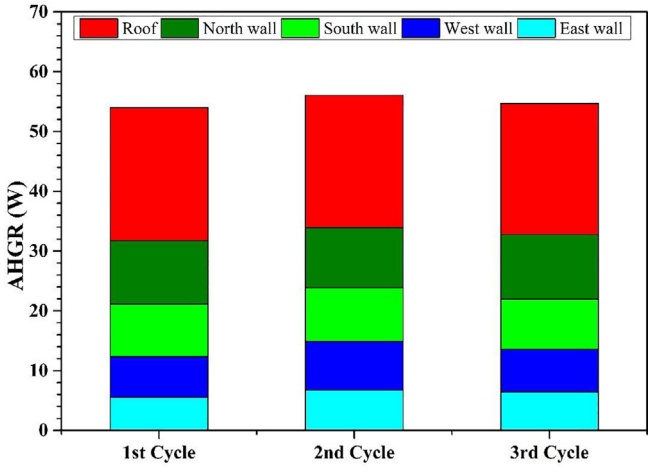

Fig. 13. AHGR in each thermal cycle.

roof) since the window-to-wall ratio was about 8.75 %, lower than 10 % [39], and were exposed to direct solar radiation for a few hours in the first half of the day. Moreover, the window HG did not consider in the HG calculations since they were similar with no PCM incorporation.

The west wall resulted in AHGR by about 6.8, 8 and 7 W in the three thermal cycles. This thermal performance is relatively good considering that west walls were exposed to solar radiation throughout the late afternoon, resulting in high inside surface temperature and long time lag with outdoor temperature compared to the other walls. From the other side, the north wall showed good AHGR by 10.6, 10 and 10.8 W, although they received low direct solar radiation during the first few hours of the day when the PCM inside the bricks is not expected to be fully melted. It should be noted that the inside surface temperature of elements interacts with each other to a limit due to limited room space. In other words, the wall exposed to high solar radiation influences the other walls that are not directly exposed to solar radiation. However, the cumulative influence of room elements directly influences the indoor temperature, indicating that the PCM room behaves better than the reference one.

In summary, considering the AHGR values of all elements during the three experimental days to the total AHGR, the descending percentage of elements contribution was 40.26 % by the roof, 19.06 % by the north wall, 15.96 % by the south wall, 13.24 % by the west wall and 11.48 % by the east wall.

3.3.2. CO_2 emission saving

Mitigating CO_2 emissions is the topmost target of modern building technologies to face the risk of global warming potential and climate change [40]. The CO_2 emission saving (CO_2 ES) in each day cycle was calculated in terms of the total AHGR and CO_2 quantity generated from each kWh power generation, according to Eq. (6) as follows:

$$CO_2ES = total\ \ AHGR \times kg\ \ CO_2/kWh\ \ electricity \times 24h \quad (6)$$

The value of 1.00284 kg CO_2/kWh electricity was taken as a standard value for Iraq according to the IEA [41], depending on the energy mixing of crude oil and natural gas sources used to generate electricity from governmental power plants. The calculation results of CO_2 ES are presented in Fig. 14.

The results presented in Fig. 14 showed that CO_2 emissions were saved by 1.3, 1.35 and 1.32 kg/day in the first, second and third experimental days. These values represent a positive contribution of PCMs in the building sector, considering the environmental impact of saved energy for long-term building service. Besides, this contribution may be maximised when considering larger envelope-enhanced PCM after proper optimisation studies to monitor the optimal PCM quantity for each element at different outside weather conditions.

3.3.3. Electricity cost saving

The electricity cost saving (ECS) is another important economic indicator since it determines the technology feasibility. The ECS, in Iraqi dinar (IQD)/day m^3, was calculated considering the total AHGR in each day and the cost of each kWh in Iraq according to Eq. (7), as follows:

$$ECS = Total\ \ AHGR \times electricity\ \ cost/kWh \times 24h \quad (7)$$

The electricity cost per kWh was taken as 60 IQD/kWh according to the latest Iraqi tariff of electricity provided to commercial buildings [42].

The calculation results of ECS each day are shown in Fig. 15, indicating ECS by 77.76, 80.64 and 78.77 IQD/day in the three experimental days. These results represent a low value in today's market compared with the initial cost of PCM and incorporation requirements. However, it will be more valuable when the long-term service of PCM for large-scale buildings is considered, along with adopting cheap and efficient PCM types with simple incorporation methods into building structure. Besides, this indicator may still be worth studying to quantify the cost saving owed to PCM incorporation for further optimisation studies in this technology.

4. Study limitations and insights for future work

The study results are limited to the examined location, which is characterised by high diurnal ambient temperature and solar radiation during the experiment. However, the same temperature trend would be expected for similar locations using PCM of high Tm with traditional thermally-poor construction materials. The thermal performance of the used PCM is also expected to be less in colder seasons (i.e., in winter and autumn) when the ambient temperature drop below the Tm of PCM. Nevertheless, the PCM could also be implemented in a way to work as a heat supplier medium during these seasons after careful optimisation consideration regarding the PCM Tm, the PCM thickness and its position within the structure.

According to the obtained results, several recommendations could be derived to be a starting point for future extended work, as follows:

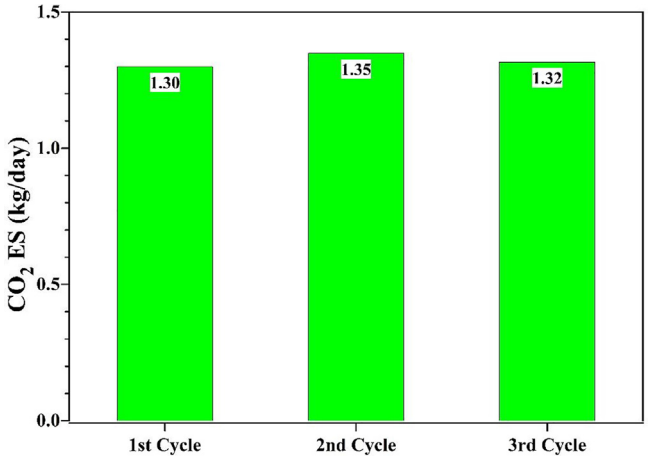

Fig. 14. CO_2 ES in each cycle.

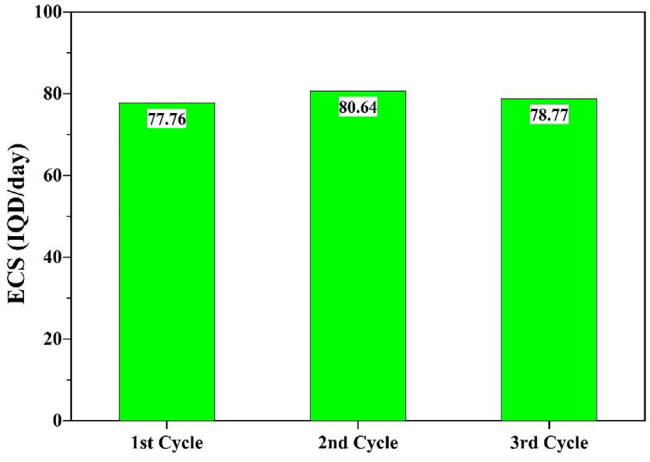

Fig. 15. ECS in each cycle.

- Some local insulations could be added to the envelope for further energy-saving in such harsh weather to attain better indoor temperature reduction and more energy saving. However, the insulation could minimise the benefits of incorporated PCM unless careful concerns are taken into consideration regarding the proper position of the insulation with respect to the PCM position.
- Recycled encapsulation materials could maximise environmental, economic and sustainable concerns.
- The PCM should be loaded in different quantities into walls depending on their orientation with respect to the sun. Accordingly, walls exposed to long-time direct solar radiation should have more PCM amount considering the wall's mechanical properties when the PCM is incorporated within bricks.
- Some active and passive techniques could be applied along with the PCM incorporation to maximise the benefits, such as thermochroic coatings, shading devices, alternative cooling mediums other than high-temperature night air, etc.

5. Conclusion

This study experimentally investigated and quantified the thermal behaviour and benefits of incorporating phase change material (PCM) into a building envelope under severe hot summer conditions in southern Iraq. Two rooms were built and examined; one incorporated PCM into the roof and brick walls, whereas the other left without PCM as a reference. The PCM room was built considering the best PCM position and quantity in the roof, and the best PCM encapsulation arrangement of bricks, according to our earlier studies. A comparison between rooms was verified by evaluating some concepts, namely the average indoor temperature reduction (AITR), thermal load levelling (TLL), average heat gain reduction (AHGR), CO_2 emission saving (CO_2 ES) and electricity cost saving (ECS). Generally speaking, even though the rooms experienced high solar radiation during the experimental period, the outcomes showed that PCM incorporation provided positive benefits. In this regard, an AITR of about 2 °C was attained with up to 8.71 % TLLR, indicating significant advances in indoor temperature. The PCM performed better with the roof than with walls due to the high PCM quantity involved and long-time exposure to high solar radiation, sharing about 40 % of the energy-saving potential. A total AHGR of up to 56 W was achieved daily, resulting in 1.35 kg/day CO_2 ES and 80.64 IQD/day ECS. These findings demonstrate the advantage of incorporating PCMs in buildings of countries that still rely primarily on traditional sources for power generation to meet energy demand, such as Iraq, intending to mitigate CO_2 emissions and save energy. However, further research perceptions are required for better performance enhancement of PCM-building applications, which end up with significant energy, environmental and economic contributions to the building sector in hot regions.

CRediT authorship contribution statement

Qudama Al-Yasiri: Conceptualization, Methodology, Data curation, Formal analysis, Investigation, Writing – original draft, Writing – review & editing. **Márta Szabó:** Conceptualization, Formal analysis, Investigation, Writing – review & editing, Supervision, Funding acquisition.

Data availability

Data will be made available on request.

Declaration of Competing Interest

The authors declare that they have no known competing financial interests or personal relationships that could have appeared to influence the work reported in this paper.

Acknowledgements

This work was supported by the Stipendium Hungaricum Scholarship Programme and Mechanical Engineering Doctoral School, MATE, Szent István campus, Gödöllő, Hungary.

References

[1] P. Nejat, F. Jomehzadeh, M.M. Taheri, M. Gohari, M.Z. Abd, Majid, A global review of energy consumption, CO2 emissions and policy in the residential sector (with an overview of the top ten CO2 emitting countries), Renew. Sustain. Energy Rev. 43 (2015) 843–862, https://doi.org/10.1016/j.rser.2014.11.066.
[2] IEA (International Energy Agency), UN Environment Programme, 2019 global status report for buildings and construction: Towards a zero-emission, efficient and resilient buildings and construction sector, 2019. https://www.worldgbc.org/news-media/2019-global-status-report-buildings-and-construction.
[3] N. Azimi Fereidani, E. Rodrigues, A.R. Gaspar, A review of the energy implications of passive building design and active measures under climate change in the Middle East, J. Clean. Prod. 305 (2021), https://doi.org/10.1016/j.jclepro.2021.127152.
[4] C. Suresh, T. Kumar Hotta, S.K. Saha, Phase change material incorporation techniques in building envelopes for enhancing the building thermal Comfort-A review, Energy Build. (2022), https://doi.org/10.1016/j.enbuild.2022.112225.
[5] T. Yan, Z. Sun, J. Gao, X. Xu, J. Yu, W. Gang, Simulation study of a pipe-encapsulated PCM wall system with self-activated heat removal by nocturnal sky radiation, Renew. Energy. 146 (2020) 1451–1464, https://doi.org/10.1016/j.renene.2019.07.060.
[6] S. Lu, B. Xu, X. Tang, Experimental study on double pipe PCM floor heating system under different operation strategies, Renew. Energy. 145 (2020) 1280–1291, https://doi.org/10.1016/j.renene.2019.06.086.
[7] D. Li, Y. Wu, C. Liu, G. Zhang, M. Arıcı, Energy investigation of glazed windows containing Nano-PCM in different seasons, Energy Convers. Manag. 172 (2018) 119–128, https://doi.org/10.1016/j.enconman.2018.07.015.
[8] J. Hu, X. (Bill) Yu, Adaptive building roof by coupling thermochromic material and phase change material: Energy performance under different climate conditions, Constr. Build. Mater. (2020), https://doi.org/10.1016/j.conbuildmat.2020.120481.
[9] M. Frigione, M. Lettieri, A. Sarcinella, Phase change materials for energy efficiency in buildings and their use in mortars, Materials (Basel). 12 (8) (2019) 1260.
[10] S. Ramakrishnan, J. Sanjayan, X. Wang, Experimental research on using form-stable PCM-integrated cementitious composite for reducing overheating in buildings, Buildings 9 (2019) 57, https://doi.org/10.3390/buildings9030057.
[11] R.A. Kishore, M.V.A. Bianchi, C. Booten, J. Vidal, R. Jackson, Enhancing building energy performance by effectively using phase change material and dynamic insulation in walls, Appl. Energy. 283 (2021), https://doi.org/10.1016/j.apenergy.2020.116306.
[12] Y. Qu, D. Zhou, F. Xue, L. Cui, Multi-factor analysis on thermal comfort and energy saving potential for PCM-integrated buildings in summer, Energy Build. 241 (2021), https://doi.org/10.1016/j.enbuild.2021.110966.
[13] E. Tunçbilek, M. Arıcı, M. Krajčík, S. Nižetić, H. Karabay, Thermal performance based optimisation of an office wall containing PCM under intermittent cooling operation, Appl. Therm. Eng. 179 (2020), https://doi.org/10.1016/j.applthermaleng.2020.115750.
[14] Y. Hamidi, Z. Aketouane, M. Malha, D. Bruneau, A. Bah, R. Goiffon, Integrating PCM into hollow brick walls: Toward energy conservation in Mediterranean regions, Energy Build. 248 (2021), https://doi.org/10.1016/j.enbuild.2021.111214.
[15] P.K.S. Rathore, S.K. Shukla, An experimental evaluation of thermal behavior of the building envelope using macroencapsulated PCM for energy savings, Renew. Energy. 149 (2020) 1300–1313, https://doi.org/10.1016/j.renene.2019.10.130.
[16] A.A.A.A. Al-Rashed, A.A. Alnaqi, J. Alsarraf, Energy-saving of building envelope using passive PCM technique: A case study of Kuwait City climate conditions, Sustain. Energy Technol. Assessments. 46 (2021), https://doi.org/10.1016/j.seta.2021.101254.
[17] M. Li, J. Shi, Mechanical and thermal performance assessment of paraffin/expanded vermiculite-diatomite composite phase change materials integrated mortar: Experimental and numerical approach, Sol. Energy. (2021) 343–353, https://doi.org/10.1016/j.solener.2021.09.014.
[18] R. Saxena, D. Rakshit, S.C. Kaushik, Experimental assessment of Phase Change Material (PCM) embedded bricks for passive conditioning in buildings, Renew. Energy. 149 (2020) 587–599, https://doi.org/10.1016/j.renene.2019.12.081.

[19] R. Ye, J. Wang, H. Jiang, N. Xie, Numerical study on thermal comfort and energy-saving potential of a prefabricated temporary house integrated with composite phase change materials, Energy Build. 268 (2022), https://doi.org/10.1016/j.enbuild.2022.112169.
[20] Z.A. Al-Absi, M.I.M. Hafizal, M. Ismail, Experimental study on the thermal performance of PCM-based panels developed for exterior finishes of building walls, J. Build. Eng. 52 (2022), https://doi.org/10.1016/j.jobe.2022.104379.
[21] Z. Ben Zaid, A. Tilioua, I. Lamaamar, O. Ansari, H. Souli, M. Hamdi Alaoui, An experimental study of the efficacy of integrating a phase change material into a clay-straw wall in the Drâa-Tafilalet Region (Errachidia Province), Morocco, J. Build. Eng. 32 (2020), https://doi.org/10.1016/j.jobe.2020.101670.
[22] N. Zhu, N. Hu, P. Hu, F. Lei, S. Li, Experiment study on thermal performance of building integrated with double layers shape-stabilised phase change material wallboard, Energy 167 (2019) 1164–1180, https://doi.org/10.1016/j.energy.2018.11.042.
[23] U. Berardi, S. Soudian, Experimental investigation of latent heat thermal energy storage using PCMs with different melting temperatures for building retrofit, Energy Build. 185 (2019) 180–195, https://doi.org/10.1016/j.enbuild.2018.12.016.
[24] Q. Al-Yasiri, M. Szabó, Case study on the optimal thickness of phase change material incorporated composite roof under hot climate conditions, Case Stud. Constr. Mater. 14 (2021) e00522.
[25] Q. Al-Yasiri, M. Szabó, Experimental evaluation of the optimal position of a macroencapsulated phase change material incorporated composite roof under hot climate conditions, Sustain. Energy Technol. Assessments. 45 (2021), https://doi.org/10.1016/j.seta.2021.101121.
[26] Q. Al-Yasiri, M. Szabó, Effect of encapsulation area on the thermal performance of PCM incorporated concrete bricks: A case study under Iraq summer conditions, Case Stud. Constr. Mater. 15 (2021) e00686.
[27] Q. Al-Yasiri, M.A. Al- Furaiji, A.K. Alshara, Comparative study of building envelope cooling loads in Al-Amarah city, Iraq, J. Eng. Technol. Sci. 51 (2019) 632–648, https://doi.org/10.5614/j.eng.technol.sci.2019.51.5.3.
[28] N.A. Habib, A.J. Ali, M.T. Chaichan, M. Kareem, Carbon nanotubes/paraffin wax nanocomposite for improving the performance of a solar air heating system, Therm. Sci. Eng. Prog. 23 (2021), https://doi.org/10.1016/j.tsep.2021.100877.
[29] H. Al-Lami, N.N. Al-Mayyahi, Q. Al-Yasiri, R. Ali, A. Alshara, Performance enhancement of photovoltaic module using finned phase change material panel: An experimental study under Iraq hot climate conditions, Energy Sources Part A Recover. Util. Environ. Eff. 44 (2022) 6886–6897, https://doi.org/10.1080/15567036.2022.2103601.
[30] M.T. Chaichan, K.I. Abaas, H.A. Kazem, Design and assessment of solar concentrator distillating system using phase change materials (PCM) suitable for desertic weathers, Desalin. Water Treat. 57 (2016) 14897–14907, https://doi.org/10.1080/19443994.2015.1069221.
[31] M.I. Hasan, Improving the cooling performance of electrical distribution transformer using transformer oil – Based MEPCM suspension, Eng. Sci. Technol. an Int. J. 20 (2017) 502–510, https://doi.org/10.1016/j.jestch.2016.12.003.
[32] M.T. Chaichan, A.H. Al-Hamdani, A.M. Kasem, Enhancing a Trombe wall charging and discharging processes by adding nano-Al2O3 to phase change materials, Int. J. Sci. Eng. Res. 7 (2016) 736–741. http://www.ijser.org.
[33] H.J. Akeiber, S.E. Hosseini, H.M. Hussen, M.A. Wahid, A.T. Mohammad, Thermal performance and economic evaluation of a newly developed phase change material for effective building encapsulation, Energy Convers. Manage. 150 (2017) 48–61, https://doi.org/10.1016/j.enconman.2017.07.043.
[34] Q. Al-Yasiri, M. Szabó, Thermal performance of concrete bricks based phase change material encapsulated by various aluminium containers: An experimental study under Iraqi hot climate conditions, J. Energy Storage. 40 (2021), https://doi.org/10.1016/j.est.2021.102710.
[35] World Weather Online. Available online: https://www.worldweatheronline.com/al-amarah-weather-averages/maysan/iq.aspx.
[36] A. Gounni, M. El Alami, The optimal allocation of the PCM within a composite wall for surface temperature and heat flux reduction: An experimental Approach, Appl. Therm. Eng. 127 (2017) 1488–1494, https://doi.org/10.1016/j.applthermaleng.2017.08.168.
[37] E. Meng, H. Yu, B. Zhou, Study of the thermal behavior of the composite phase change material (PCM) room in summer and winter, Appl. Therm. Eng. 126 (2017) 212–225, https://doi.org/10.1016/j.applthermaleng.2017.07.110.
[38] H.-F. ASHRAE, Chapter 22, Thermal and Moisture Control in Insulated Assemblies—Fundamentals, Am. Soc. Heating, Refrig. Air-Conditioning Eng. Inc., Atlanta. (1997).
[39] H. Alibaba, Determination of optimum window to external wall ratio for offices in a hot and humid climate, Sustainability 8 (2016) 187, https://doi.org/10.3390/su8020187.
[40] M.Ç. Uludaş, E. Tunçbilek, Ç. Yıldız, M. Arıcı, D. Li, M. Krajčík, PCM-enhanced sunspace for energy efficiency and CO2 mitigation in a house in mediterranean climate, J. Build. Eng. 57 (2022), https://doi.org/10.1016/j.jobe.2022.104856.
[41] International Energy Agency, Data and statistics: CO_2 emissions. Available online: https://www.iea.org/data-and-statistics/data-browser?country=IRAQ&fuel=CO2 emissions&indicator=ElecIndex.
[42] Iraq electricity prices. Available online: https://www.globalpetrolprices.com/Iraq/electricity_prices/#:~:text=Iraq%2C December 2021%3A The price,of power%2C distribution and taxes.